Journal of Contaminant Hydrology 267 (2024) 104425

Contents lists available at ScienceDirect

Journal of Contaminant Hydrology

journal homepage: www.elsevier.com/locate/jconhyd

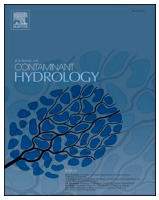

PFOA remediation from kaolinite soil by electrokinetic process coupled with activated carbon/iron coated activated carbon - permeable reactive barrier

Namuun Ganbat [a,b], Ali Altaee [a,*], Faris M. Hamdi [a], John Zhou [a], Mahedy Hasan Chowdhury [a], Syed Javaid Zaidi [c], Akshaya K. Samal [d], Raed Almalki [a], Marie Joshua Tapas [e]

[a] Centre for Green Technology, School of Civil and Environmental Engineering, University of Technology Sydney, 15 Broadway, NSW 2007, Australia
[b] Photon Remediation, 219-241 Cleveland, St Redfern, NSW 2016, Australia
[c] UNESCO Chair in Desalination and Water Treatment, Center for Advanced Materials, Qatar University, Doha, Qatar
[d] Centre for Nano and Material Sciences, Jain University, Bangalore, 562112, India
[e] School of Civil and Environmental Engineering, University of Technology Sydney, 15 Broadway, NSW 2007, Australia

ARTICLE INFO

Keywords:
PFOA remediation
Soil decontamination
Electrokinetic
Surfactant enhancement

ABSTRACT

This study applied electrokinetic (EK) in situ soil remediation for perfluorooctanoic acid (PFOA) removal from kaolinite soil. The kaolinite soil was spiked with 10 mg/kg PFOA for the EK treatment using Sodium Cholate bio-surfactant coupled with Activated Carbon (AC) or iron-coated Activated Carbon (FeAC) permeable reactive barrier (PRB). The study also evaluated the impact of AC and FeAC PRBs' position on the EK process performance. In the EK with the PRB in the middle section, PFOA removal from kaolinite was 52.35 % in the AC-EK tests and 59.55 % in the FeAC-EK. Experimental results showed the accumulation of PFOA near the cathode region in FeAC PRB tests, hypothesising that Fe from the PRB formed a complex with PFOA ions and transported it to the cathode region. Spent PRBs were regenerated with methanol for PFOA extraction and reuse in the EK experiments. Although FeAC PRB achieved better PFOA removal than AC PRB, the EK tests with regenerated AC-EK and FeAC-EK PRBs achieved 40.37 % and 20.62 % PFOA removal. For EK with FeAC PRB near the anode, PFOA removal was 21.96 %. Overall, using PRB in conjunction with the EK process can further enhance the removal efficiency. This concept could be applied to enhance the removal of various PFAS compounds from contaminated soils by combining a suitable PRB with the EK process. It also emphasizes the feasibility of in-situ soil remediation technologies for forever chemical treatment.

1. Introduction

Ineffective waste management, industrial activity, urbanisation, commercial plantations, and mining all contribute to soil contamination. In recent years, perfluorooctanoic acid (PFOA)-contaminated land has become an emerging environmental issue. The contamination of soil has a significant effect on the environment, living organisms, and ecosystems. PFOA is one of the most prevalent *per*- and polyfluoroalkyl substances (PFAS) compounds detected in the environment. A strong C—F covalent bond endows PFOA compounds with unique and potent physicochemical properties. The PFOA compound's hydrophobic chain and hydrophilic head account for their water and oil-repellent properties. Due to its physicochemical properties, PFOA is widely used in non-stick cookware, surface sprays, and firefighting foams. Since PFOA is non-biodegradable, persistent, and accumulates in the environment, the soil becomes an enormous sink for PFOA contamination. Although PFOA-containing products have been phased out and banned in many countries, PFOA-contaminated land remains a major environmental issue. Primary sources of PFOA contamination include fire training lands such as airports, military sites, and PFOA production sites. The secondary pollution sites are mainly pathways that produce by-products containing PFOA (Epa Au, 2019).

In 2009, PFAS compounds were added to the Stockholm Convention on Persistent Organic Pollutants as a pollutant of concern (European C, 2020). This convention is an agreement to protect humans and the environment from persistent organic pollutants. In accordance with this

* Corresponding author.
E-mail address: ali.altaee@uts.edu.au (A. Altaee).

https://doi.org/10.1016/j.jconhyd.2024.104425
Received 12 May 2024; Received in revised form 3 September 2024; Accepted 4 September 2024
Available online 5 September 2024

convention, chemicals are subject to restriction and elimination. Since 2012, the Australian government has been a member of the United Nations Environment Program/Organisation for Economic Co-operation and Development (OECD/UNEP) Global Perfluorinated Chemicals Group (European C., 2020). The group works to reduce and eliminate products containing PFAS. Therefore, several nations phased out the production and use of PFOA-containing products (Lenka et al., 2021).

Because PFOA soil contamination is an emerging environmental issue, several remediation studies for contaminated sites are still experimental (Mahinroosta and Senevirathna, 2020). Thermal heating is one of the most prevalent physical remediation techniques used to clean up PFAS-contaminated sites (Altarawneh et al., 2022). Thermal heating is an energy-inefficient, costly, and destructive method that involves heating the contaminated soil at 1500 K (1226 °C), resulting in industrial waste. Consequently, less environmentally damaging methods are preferred. Lab-scale stabilization and solidification tests on PFAS-contaminated firefighting training soils demonstrated that granular activated carbon has a greater sorption capacity to PFAS than activated carbon-clay blend, modified clay, and biochar (Barth et al., 2021). Planetary ball milling has been studied as a mechanochemical remediation technique for AFFF-contaminated soils; it reduced PFOA and PFOS in dry sand by 99 and 98 % (Turner et al., 2021). The electrochemical destruction of PFOA and PFOS was studied on a lab scale, and the results indicated 51.7 and 33.3 % degradation, respectively (Hou et al., 2022).

Electrokinetic remediation is a well-known method for removing heavy metals from soil. It involves passing a low-density direct electric current through soil, transporting the contaminants between electrodes (anodes and cathodes) placed at appropriate distances (Virkutyte et al., 2002). Electrokinetic remediation for contaminated soils aims to remove contaminants from low-permeability soils under the influence of a low-level direct current, with electroosmosis, electromigration, and electrophoresis as the primary transport mechanisms (Acar and Alshawabkeh, 1993). The transport of contaminants towards the electrode of opposite charge increases when dissolved charged particles are in the interstitial fluid. The contaminants are then collected in the chambers of one of the electrodes and disposed of appropriately. Most hydrophobic organic particles are nonionic and unaffected by an electrical field (Cheng et al., 2017). Successful remediation of persistent organic pollutants is challenging, and their removal using conventional techniques, such as soil stabilization and solidification and chemical treatment, is difficult. Various studies have recently used enhanced electrokinetic processes to increase the efficiency and productivity of the electrokinetic (EK) system. Recent studies demonstrated the effects of different surfactants as enhancing agents for removing PFOA-contaminated kaolin (Ganbat et al., 2022). The research findings demonstrated the most effective surfactant as enhancing agent was the sodium cholate enhanced EK system which resulted in the highest removal rate of PFOA.

EK remediation in conjunction with a permeable reactive barrier (PRB) has attracted the interest of researchers due to its effective application and increased EK efficiency. PRB-assisted remediation technologies are passive remediation systems designed specifically to remove hydrophobic organic compounds and heavy metals from soil (Li et al., 2011). PRB enhances EK soil remediation technologies by capturing contaminants and decreasing their concentration in anolyte and catholyte chambers (Ghobadi et al., 2020). Numerous PRB types are utilized in EK systems according to their absorption mechanisms, cost-effectiveness, and lifetime. Commonly employed PRBs include biochar, activated carbon (AC), and biomaterials. The application of biological PRB-enhanced EK remediation to remove diesel-contaminated clay was investigated on a lab scale (Mena et al., 2016). The results indicated a successful increase in electroosmotic flow and a promising performance for future in-situ applications. The application of compost as a PRB in an EK system for removing copper from contaminated soil was successful in a laboratory setting, resulting in a removal rate of over 90 % (Ghobadi et al., 2020). The removal of cadmium using array electrode EK with PRB was evaluated, and the average removal rate was 93.1 % (Zhou et al., 2020). Numerous applications of EK enhanced with PRB for eliminating inorganic and organic contaminants have been proven effective (Li et al., 2011; Ghobadi et al., 2020; Mena et al., 2016; Zhou et al., 2020; Ruiz et al., 2014).

Activated carbon (AC) derived from coal and other carbon-rich materials has a distinctive physicochemical structure, a large surface area, and a well-developed porous structure, making it an ideal candidate for the adsorption of contaminants from water and soil. Hydrophobic interactions and electrostatic attractions are the primary adsorption mechanisms for PFAS on AC. Hydrophobic properties of PFOA permit a high adsorption capacity on AC, given that hydrophobicity is the predominant adsorption mechanism for AC. Granular activated carbon (GAC)-PRB-enhanced EK was studied to remove Tricresyl phosphate (TCP)-contaminated clay, and more than 80 % of the TCP was successfully removed (Ruiz et al., 2014). GAC impregnated with iron oxide has high adsorption efficiency for removing heavy metals and organic contaminants, as it has a good binding capacity. It has been studied extensively to remove hazardous contaminants from wastewater (Kim et al., 2010; Suresh Kumar et al., 2017a). Combining iron-coated charcoal (Fe/C) PRB with EK is promising and efficient for removing persistent organic pollutants (Sun et al., 2017). Niarchos et al. (Niarchos et al., 2023) conducted a pilot plant test using colloidal activated carbon (CAC) to stabilize PFAS in the soil and achieved outstanding removal of perfluorooctane sulfonic acid and perfluorooctanoic acid. Another Study by Ganbat et al. (Ganbat et al., 2023) achieved 94 % PFOA removal from kaolinite soil using a combined 70 %–30 % iron slag-activated carbon PRB with the EK process. Mass balance results showed that 87 % of the PFOA in the soil accumulated in the PRB, and the remaining 7 % PFOA concentration was in the anolyte and catholyte.

This study evaluated sodium cholate biosurfactant-enhanced EK, combined with AC and FeAC PRB, to remove PFOA from contaminated soil to the PRB and catholyte. Our previous study demonstrated the high efficiency of sodium cholate biosurfactant for PFOA removal from the kaolinite soil (Ganbat et al., 2022). The effectiveness of AC and FeAC as PRB in the EK system and their post-regeneration performance were investigated. Although electrochemical studies for the degradation of PFAS compounds were conducted in the past, the combination of surfactant-enhanced EK and PRB for removing PFOA-contaminated soils has not been reported. The Ek experiments were conducted for two weeks at 20 mA electric potential to compare PFOA removal by different PRBs.

2. Materials and methods

2.1. Materials, soil preparation, and analysis

PFOA with a purity >99 % was purchased from Sigma-Aldrich, Australia. PFOA was selected to represent PFAS contaminants because it is a common PFAS compound that has been frequently reported in the literature (Brusseau et al., 2020). Due to its low permeability, low carbon content, and poor cation exchange capacity, kaolin clay purchased from Keane Ceramic Pty. (Australia) was selected as the model soil for

Table 1
Physico-chemical properties of kaolinite soil and PRBs.

Parameters	Soil	AC/PRB	FeAC/PRB
Particle size analysis	46.81	100 mesh	100 mesh
Clay	51.17	NA	NA
Sand/Silt	2.02	NA	NA
Permeability (m/s)	4×10^{-10}	1.11×10^{-3}	1.67×10^{-3}
Density (g/cm^3)	1.45	1.48×10^{3}	1.26×10^{3}
Porosity (kg/m^3)	633	950	146.57
Organic matter	Negligible	NA	NA
TDS (mg/L)	145	NA	NA
pH	5.24 ± 0.03	5.25	5.93
Electrical conductivity (mS/cm)	0.46	4.14	5.50

the EK tests. The physicochemical characteristics of the kaolin soil used in the EK tests are presented in Table 1. The kaolin soil was spiked with PFOA for all EK experiments with a 10 mg/kg target concentration. 1 g of PFOA was dissolved in 1000 mL of DI water, and the solution was then diluted to 10 mg/L. Approximately 1000 g of kaolin was combined for each experiment with 10 mg/L of PFOA solution. Consistent distribution and homogeneous PFOA adsorption were achieved by maintaining the spiked soil at room temperature for at least 72 h and stirring it frequently. As PRB, (70 g) AC (100 mesh) purchased from Sigma-Aldrich in Australia was used for each experiment. Iron (III) Sulphate and Potassium Permanganate were purchased from Sigma Aldrich in Australia to modify AC. The saturated soil was then layered into the reactor and compacted uniformly to ensure the uniform distribution of PFOA. A multimeter (model HACH HQ40D) was used to measure the soil's pH and electrical conductivity by making slurries with a dry soil-to-water ratio of 1:5 (w:v) (Altaee et al., 2008). Before and after EK tests, the PFOA concentration in soil was analysed using LC-MS (SHIMADZU, Japan) as an analytical instrument.

2.2. Iron coating of AC

FeAC PRB was made using a modified version of a method that has been published (23,20). The AC was washed with DI water to get rid of any surface pollutants, and it was then dried for 4 h in an oven at 105 °C. In the meantime, 0.5 M $KMnO_4$ solution was prepared and mixed with AC for 12 h. The oxidised AC was filtered, washed thoroughly, and dried in the oven at 105 °C. 10 % m/m $Fe.Cl_3.6H_2O$ solution and oxidised AC were added, and the slurry was mixed at 250 rpm for 12 h to create FeAC. The mixture was filtered, washed with DI water, and dried at 105 °C in the oven. The surface modification of FeAC was then analysed using a BET analyser and SEM-EDS.

2.3. Electrokinetic cell setup and test design

The EK reactor comprises two electrode compartments at either end: a soil compartment, a PRB compartment, and an electrolyte reservoir (Fig. 1). In experiments T2 to T5, 2 cm PRB was sandwiched between two filter papers in the middle of the soil compartment, whereas the PRB was placed near the anode in experiment T6 to study the impact of PRB position on PFOA removal by the EK process (Table 2). Filter paper (5–13 μm LLG) Labware supported by a perforated plexiglass plate was placed between the electrode chamber and the soil compartment to prevent soil from entering the electrolyte chambers. At the end of the T2 to T5 tests, the soil was divided into equal sections, S1 to S6, from the anode to the cathode, with PRB in the middle. On the contrary, the PRB was next to the anode in the T6 test, followed by the soil sections S1 to S6

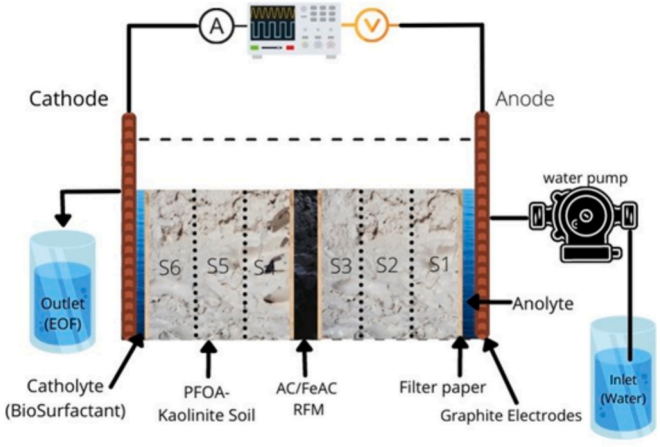

Fig. 1. Electrokinetic setup used in the soil remediation process.

from the anode to the cathode.

A constant current was applied using a DC bench power supply (EA-PS 3016-10B, EA Electro-Automatik), and the electric current and voltage were measured and recorded hourly using a multimeter (Keithley 175 Autoranging multimeter). The electrode chambers on either side of the reactor were equipped with two (15 × 1 cm) graphite rod electrodes (Graphite Australia Pty Ltd). Based on the results of the previous study, the biosurfactant NaC was added to the catholyte solution (Sigma-Aldrich). NaC outperformed conventional surfactants in enhancing PFOA removal in the EK process (Ganbat et al., 2022). Regular injections of ultra-pure water were made into the anolyte compartment to make up for water loss brought on by electroosmotic flow. Throughout the experiment, electroosmotic flow and current intensity were periodically measured.

The EK experiments were conducted at room temperature without pH control with an initial steady current of 20 mA. Table 2 provides details on the six EK experiments. The anolyte was MQ water, and the catholyte was a 5 % (*w*/w) NaC biosurfactant. The fluid level in the inflow reservoir was maintained at a constant level to maintain a continuous hydraulic gradient throughout the soil. The EK test was carried out for two weeks using PFOA-contaminated kaolin soil with an initial 10 mg/kg concentration.

A series of experiments were conducted to assess the effectiveness of the PRB-enhanced EK process. The first experiment, referred to as T1, served as a reference to examine the removal of PFOA without the presence of a PRB. During this test, only a 5 % wt NaC biosurfactant was introduced at the cathode. In T2, the efficacy of activated carbon (AC) PRB coupled with the NaC biosurfactant was investigated. Similarly, T3 focused on the effects of an iron-loaded AC (FeAC) PRB coupled with the biosurfactant. For experiments T2 and T3, the PRBs were placed in the middle of the soil compartment, and a fixed electrical current of 20 mA was applied. Experiments T4 and T5 explored the efficiency of RFM-EK with the regenerated AC and FeAC PRBs, respectively. The regenerated PRB in experiment T4 was recycled from experiment T2 after PFOA extraction at the end of experiment T2, whereas in experiment T5, it was recycled from experiment T3. These PRBs were recovered through methanol extraction and then reused in subsequent tests. Additionally, experiment T6 examined the impact of placing the FeAC PRB near the anode.

2.4. PFOA analysis

The power supply was disconnected at the conclusion of fourteen days, and the experimental setup was dismantled. Aqueous solutions from both the anode and cathode chambers were collected, and perfluorooctanoic acid (PFOA) concentrations, pH levels, and electrical conductivity (EC) were assessed. The soil specimen was divided into six equal sections, carefully extruded and mixed homogenously, and then dried overnight at 1050C in an oven. 5 g of dried soil was taken in duplicate from each section. PFOA content was measured by triple methyl alcohol extraction, where 5 mL of methyl alcohol was put into 5 g dried soil, shaken on a flat shaker at 180 rpm and 220C for 60 min, sonicated at 300C for 30 min, and centrifuged at 8000 rpm for 10 min. After three extractions, the supernatants were mixed, diluted, and filtered (PTFE syringe filter) and transferred into vials for LC-MS analysis (LC/MS 8060, Shimadzu, shim pack column 1.6 μm, 2.0 mm × 50 mm). (Zhan et al., 2020). PRB was also extracted in the same way as soil samples. The following equation was used to determine the removal efficacy:

$$\text{Removal efficiency } (\%) = \frac{C_0 - C_f}{C_0} \times 100 \quad (1)$$

In the equation above, C0 and Cf are PFOA (mg/kg) concentrations initially and after EK treatment in the soil sections (S1-S6 and PRB).

A calibration curve was prepared using a series of PFOA standards at concentrations ranging from 0.2 mg/L to 50 mg/L. Calibration checks

Table 2
Overview of electrokinetic experiments and their parameters. NaC: sodium cholate, AC: activated carbon, FeAC: iron-loaded activated carbon.

Exp No.	Target Contamination	Concentration of PFOA (mg/kg)	Surfactant and dosing point	PRB type and position	Surfactant Concentration (% *w*/w) Catholyte	Duration (days)
T1	PFOA	10	NaC/cathode	NA	5	14
T2	PFOA	10	NaC/cathode	AC in the middle	5	14
T3	PFOA	10	NaC/cathode	FeAC in the middle	5	14
T4	PFOA	10	NaC/cathode	Regenerated AC in the middle	5	14
T5	PFOA	10	NaC/cathode	Regenerated FeAC in the middle	5	14
T6	PFOA	10	NaC/cathode	FeAC at the anode	5	14

were performed at the beginning, middle, and end of each analytical batch to ensure instrument accuracy and precision. Acceptable calibration check recoveries ranged from 80 % to 120 %. Method blanks were processed with each batch of samples to monitor for potential contamination during sample preparation and analysis. PFOA concentrations in method blanks were below the detection limit, indicating no significant contamination. Matrix spike samples were prepared by adding a known quantity of PFAS standards to pre-extracted soil samples. Recovery rates for matrix spikes were calculated to assess method accuracy and ranged from 80 % to 110 %.

A 1:5 (*w/v*) ratio of dry mass to DI water slurry was prepared to measure the pH and EC of the soil and the PRB. HACH HQ 11D model pH and electric conductivity meter were used for all the measurements. The Zeta potential of PRB was measured before and after the EK test. BET analyser was used to measure the surface area of AC before and after the iron loading procedure. SEM coupled with EDS was used to analyse the surface characteristics of AC-PRB and FeAC PRB before and after the EK test and after the reused EK experiment. For quality control in FTIR, pure KBr was used as a background to eliminate spectral interferences, and the instrument was calibrated with standard compounds for accurate wavenumber measurements. SEM-EDX involved regular calibration of detectors with standard reference materials and the use of control samples with known morphology and elemental composition for validation. Zeta-potential analysis included the use of standard reference materials for calibration and triplicate measurements for reproducibility and accuracy. For BET analysis, the analyser was calibrated with standard materials with known surface areas, and repeated measurements were conducted to ensure data consistency and reliability.

3. Results and discussion

3.1. Electrical current

The applied current is one of the most important variables in the electrokinetic test as it controls the fate of contaminants in the soil medium under a direct electric field. Fig. 2 presents the electric current and voltage variation over time for the EK tests. The applied electric current in this study was 20 mA. However, the applied current in all EK tests decreased with increased elapsed time to a final value below 5 mA. The electrolysis reaction that generates hydrogen ions at the anode and hydroxide ions at the cathode under the applied current causes the current to rise at the beginning of the EK test. This increase in current is related to the increase in additional mineral dissolution (Hahladakis et al., 2016). Generation of the acid front at the anode and solubilisation of free ions in the soil induces ions to electromigrate to the electrodes (Ghobadi et al., 2020). As shown in Fig. 2a, the current surged at the start of the experiment and remained constant for several hours before gradually decreasing. The pattern of change in current over time in EK testing for removing PFOA is consistent with previous studies (Ganbat et al., 2022). This phenomenon may be caused by PFOA migration and accumulation in the soil, which increases soil pore resistance and reduces the electrical current. A similar change in the electric current was observed in a bench-scale study that used FeC PRB EK to remove

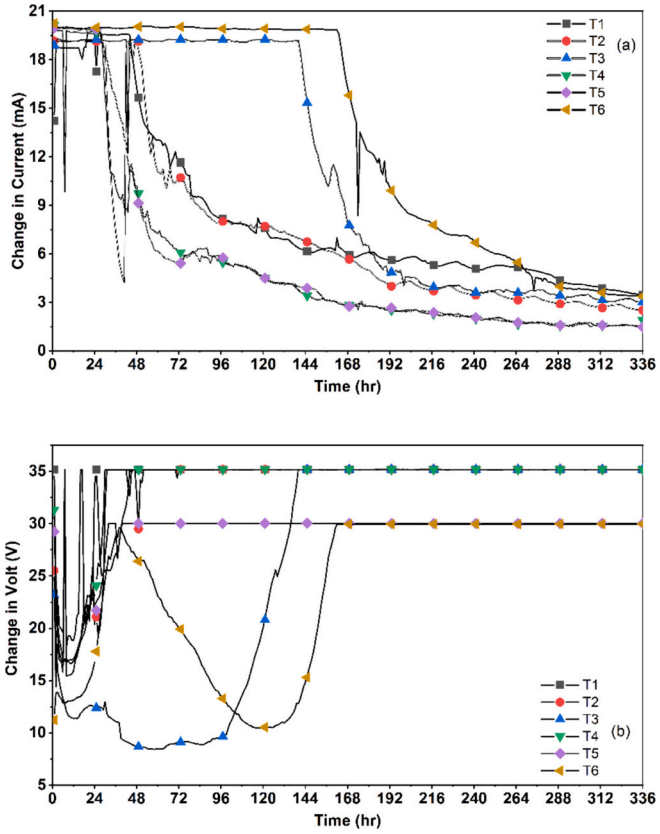

Fig. 2. Change in current of all experiments after 2 weeks.

phenanthrene from contaminated soil and EK tests for removing copper ions from contaminated soil (Ghobadi et al., 2020; Ren et al., 2019).

As shown in Fig. 2a, EK tests were constant at 20 mA for at least 48 h before they began progressively declining. In experiment T1, the electric current remained steady at 20 mA for 44 h, eventually decreasing to 3.48 mA at the end of the EK test. The electric current in experiment T2 was steady for 50 h and then dropped to 2.51 mA after 336 h. However, experiments T3 and T6 remained steady at about 20 mA for 144 and 168 h, respectively. The prolonged constant current in the FeAC PRB experiments is accountable for the Fe ion's presence on the AC surface. At the end of the EK test, the electric current in experiments T4 and T5 using recycled PRB gradually decreased to 1.9 mA and 1.49 mA after remaining constant for 27 h.

FeAC-EK tests had higher average electric currents than AC-EK tests; T3 and T6 were 11.0 mA and 13.23 mA, respectively, whereas the AC-EK test had an average electric current of 7.21 mA. Experiment T3 with FeAC PRB exhibited a higher electric current than T2 and T5 experiments with AC PRB due to i) the electric conductivity of FeAC being higher than that of the AC PRB, ii) the propagation of acid front in the soil caused the dissolution of iron ions and migration towards the

cathode zone and iii) the formation of a complex of PFOA with Fe^{3+} result in the transportation towards the cathode. Interestingly, the electric current profile in experiment T5 was similar to that in experiments T2 and T4, indicating that most Fe coating film on the AC was lost during the EK and regeneration processes. Experiment T4 with regenerated AC exhibited the lowest average electric current of 5.14 mA, followed by experiment T5 with regenerated FeAC of 4.31 mA.

Ions precipitation and convergence of acid and alkaline fronts in the soil increase soil resistivity to electric current and hence the electric potential. Fig. 2b shows an increase in the electric potential of all experiments after 30 to 150 h. For example, the average electric potential in experiment T6 was 24.09 *V* and 26.14 V in experiment T3. In contrast, the average electric potential in experiment T4 was 33.9 V and 29.18 V in experiment T5, indicating early metal ions precipitation or acid and alkaline front convergence in the soil. Generally, the electric potential in the EK experiments increased slowly over time due to increasing soil resistivity. Finally, it reached a constant value and remained constant until the end of the EK experiments (Fig. 2b).

3.2. Soil pH and electric conductivity

The effective ionic mobility of the hydrogen ion under an electric field is approximately 1.8 times higher than that of hydroxyl ion; this allows hydrogen ions to sweep across the soil faster. As a result, acidic pH predominates in soil sections. The diffusion coefficients for H^+ and OH^- are relatively high, and their dissociation factor in water is also high and rapid; consequently, their electromigration defines the soil chemistry (Figueroa et al., 2016). As shown in Fig. 3a, the soil pH was

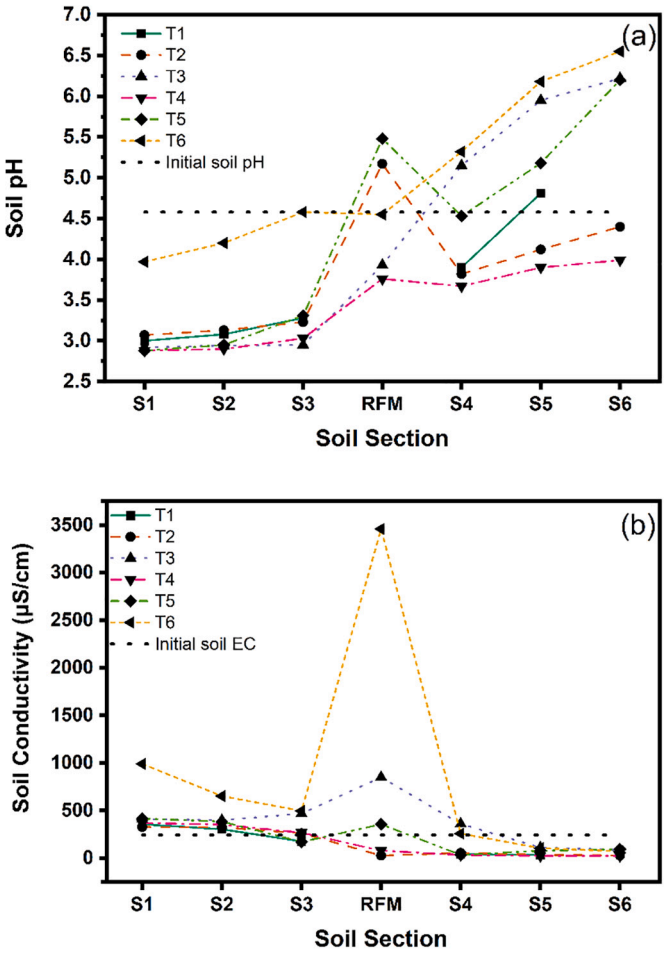

Fig. 3. (a) pH across the soil section of different EK tests (b) electric conductivity of the soil sections for all EK tests.

acidic, i.e., < pH 7, in soil sections 1 to 6 due to the rapid advancement of the acid front from the anode to the cathode. In experiments T1, T2, and T4, soil pH remained below the initial pH of 4.7 due to acid propagation from the anode to the cathode. In contrast, the soil pH in experiments T3, T5, and T6 was below the initial soil pH in sections S1 to S3, the increased over the initial soil pH in sections S4 to S6 due to the advancement of alkaline from the cathode to the anode zone. Experiments T3, T5, and T6 with FeAC PRB could cause a slight increase in the initial soil pH due to the formation of iron hydroxide after iron migration towards the cathode zone.

In experiment T1, the pH values in sections S1 through S3 were 3.00, 3.08, and 3.28, then slightly increased to pH 3.9 in section S4 before rising to pH 4.84 in section S5. As portrayed in Fig. 3a, there is an insignificant change in sections S1 to S3 pH of experiments T1 to T5; soil pH increased in sections S4 to S6 closer to the cathode region. The inconsistency in soil pH of experiments T1 to T6 is due to the application of different PRB types. Experiment T6 had the highest overall soil pH, between pH 3.96 and 6.55. As mentioned before, experiments with FeAC PRB exhibited higher soil pH, especially in soil sections close to the cathode, due to the formation of iron hydroxide caused by iron ions leaching from the FeAC PRB. Technically, low pH increases PFOA sorption in soils with high contents of sesquioxides (Fe and Al oxides) (Oliver et al., 2019). Nevertheless, the experimental findings imply that pH levels are not directly correlated with PFOA accumulation or removal rates in kaolinite soil.

One of the key components of EK is the soil's electric conductivity (EC), which measures the soil pore fluid's ability to carry electric current and is determined by ion concentration in the soil water. The EC and the soil pH are inversely correlated (Fig. 3b). Water hydrolysis at the anode generates H^+ ions, increasing the anode's electric conductivity. The soil EC showed a progressive reduction from the anode to the cathode region, indicating that more free ions are in the anode than in the cathode region. According to experimental data, EC values peaked in section S1 and then dropped gradually over the soil sections towards the cathode zone. As anticipated, the low EC in soil sections close to the cathode is caused by the precipitation of metal ions in the alkaline environment. As shown in Fig. 3b, the EC of non-PRB-EK and AC PRB were lower than that of FeAC. The presence of the iron film on the AC surface may be responsible for these findings. The soil's conductivity and ions content rose due to the micro-electrolysis of Fe close to the PRB (Chen et al., 2007; Yan et al., 2013); these results are in accordance with the soil's pH. Previous studies have supported the inversely associated relationship between soil pH and EC, the low pH in sections in the anode region, and a gradually increasing inclination towards the cathode section (Ghobadi et al., 2021; Andrade and dos Santos, 2020; Guedes et al., 2019).

3.3. Removal of PFOA

Based on the PRB used in the EK tests, the residual concentration of PFOA in soil sections exhibited a fluctuated distribution (Fig. 4a). During the EK process, PFOA was mainly transported by electroosmosis and electromigration (Guedes et al., 2019). Sodium cholate (NaC) biosurfactant was added to the catholyte in all EK experiments to facilitate the transportation of PFOA. NaC promotes PFOA dissolution into surfactant micelles, enhancing the removal efficiency and PFOA-containing micelle transport. The environmental biocompatibility of NaC, low micelle aggregation number, and low critical micelle concentration contributed to its selection as an enhancement agent (Sugioka et al., 2003). In a previous study, NaC demonstrated a superior removal rate to conventional surfactants, e.g., Tween 80 and sodium dodecyl sulphate (SDS) (Ganbat et al., 2022). As anticipated in a non-PRB enhanced EK experiment T1, PFOA accumulated in the middle section S3, as illustrated in Fig. 4a. Due to electroosmotic flow going in the cathode's direction and PFOA anion electromigration towards the anode direction, PFOA accumulated in the middle of the EK cell. The findings of another

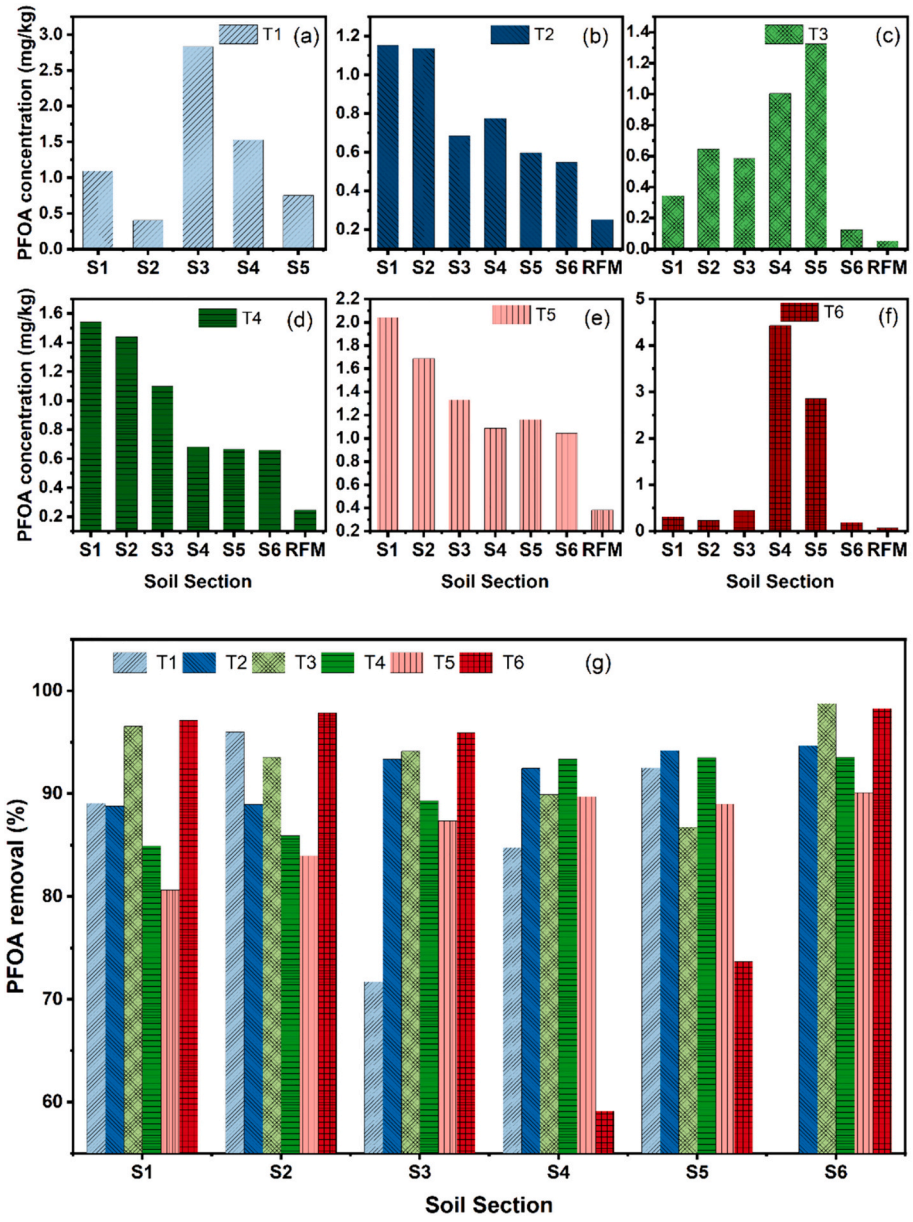

Fig. 4. PFOA distribution in soil sections after remediation in (a) T1, (b) T2, (c) T3, (d) T4, (e) T5, (f) T6; (g) PFOA removal rate in soil sections post-treatment.

lab-scale electrochemical investigation have validated a similar PFOA transportation pattern (Hou et al., 2022).

As PFOA accumulated in the middle of the EK cell, PRB was positioned there in experiment T2 to optimize the removal of PFOA during the EK process. PFOA content in soil sections exhibited a decreasing tendency towards the cathode region in experiment T2 (AC-PRB), as depicted in Fig. 4b. The concentration of PFOA was 1.15 mg/kg near the anode in section S1 and then slightly dropped to 0.546 mg/kg near the cathode in section S6. The PRB contained 0.253 mg/kg of PFOA at the end of the EK test. Iron-coated AC (FeAC) PRB was used in the middle section in experiment T3 and at the anode in experiment T6 to capture PFOA in the soil to study the impact of FeAC PRB on PFOA removal.

Previous research findings have demonstrated that FeAC exhibits a significantly higher adsorption capacity when compared to AC in aqueous medium (Ahn et al., 2022). As presented in Fig. 4c and f, the PFOA concentrations were lowest in section S1 (circa 0.34 mg/kg), dramatically increased in sections S4 and S5, and then decreased to 0.125 mg/kg in section S6. In experiments T3 and T6, the PFOA concentration increased near the cathode in sections S4 and S5, probably due to the PFOA adsorption on iron hydroxide that was dissolved from the FeAC PRB by the advancement of the acid front from the anode to the cathode and carried by the electroosmosis flow towards the cathode. The EDS results show Fe and O in the FeAC PRB before and after the EK process, confirming the theory of PFOA adsorption on the iron oxide that migrated towards the cathode (Fig. 5).

As depicted in Fig. 4d and e, reused PRB in experiments T4 and T5 exhibited a similar trend of PFOA distribution across soil sections after the EK process. The following PFOA concentrations were found in experiment T4, 1.5413 to 0.2458 mg/kg in sections S1 to S6. Likewise, experiment T5 showed a declining tendency towards the cathode, with PFOA concentrations of 2.038 to 0.383 mg/kg in sections S1 to S6. Given the high concentration near the anode, electromigration likely served as the main mechanism for migrating PFOA anion in experiments T2, T4, and T5. Although experiment T5 used a regenerated FeAC, the experiment showed an AC-PRB-like pattern. Following the first cycle of the EK test and throughout the regeneration process, it is likely that some Fe was dissolved in the low pH and migrated to the cathode. In experiment T6, the FeAC was placed near the anode to study the impact of the PRB

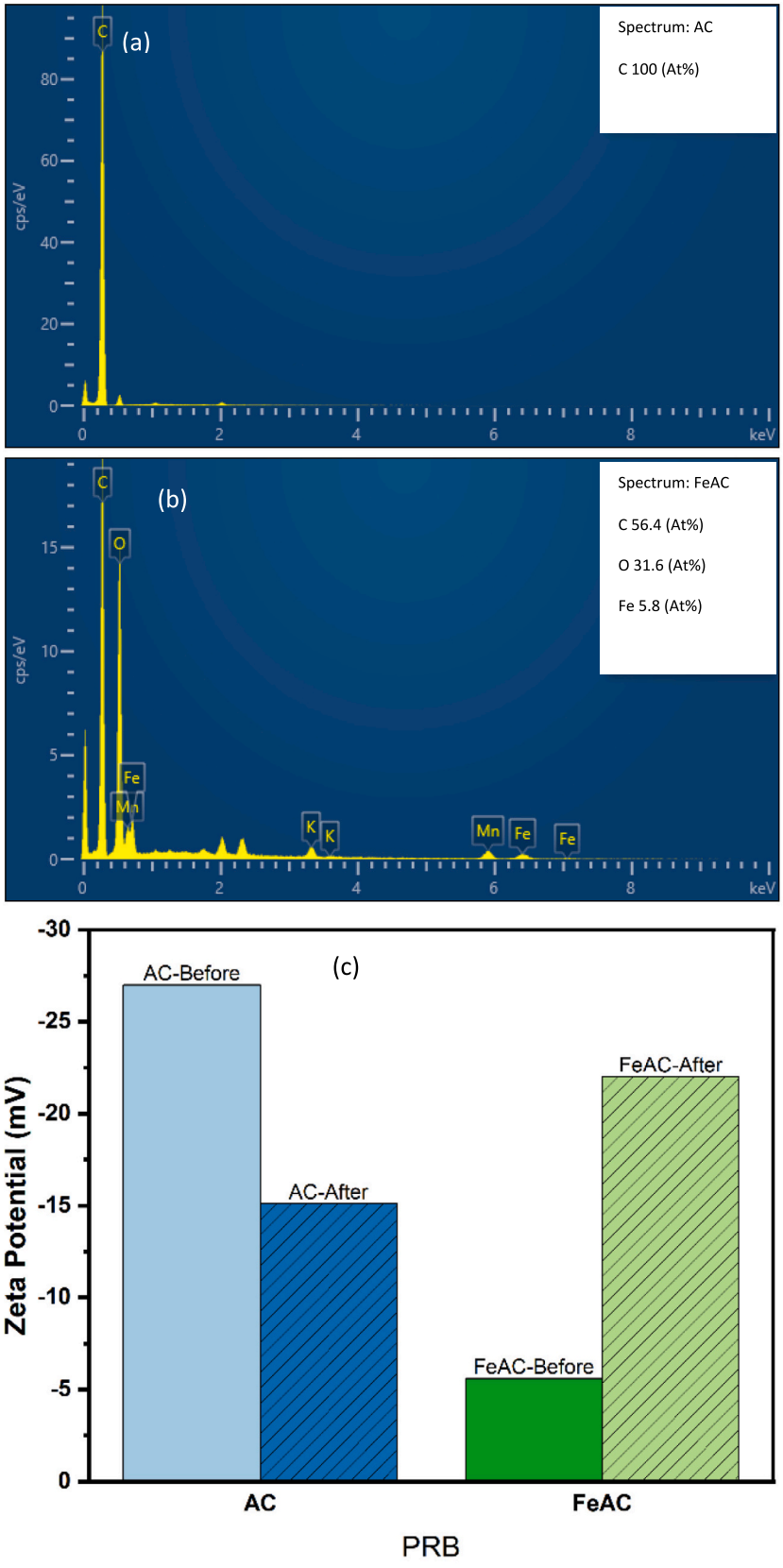

Fig. 5. (a) AC EDS (b) FeAC EDS after iron loading (c) Zeta Potential of AC and FeAC PRB before and after EK tests (d) FTIR results of AC, FeAC before and after EK.

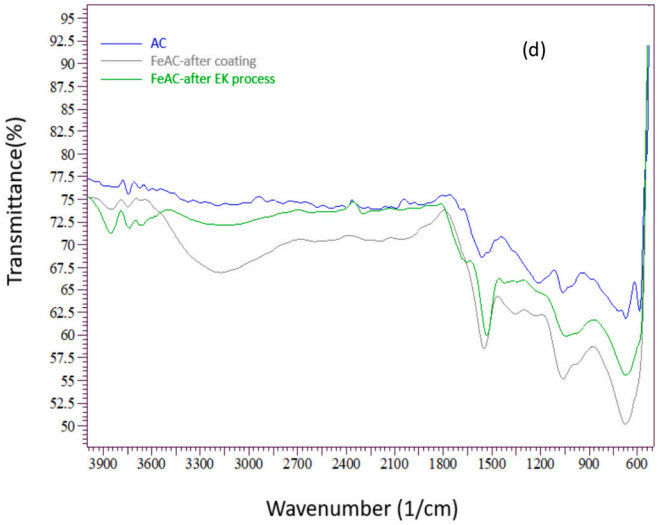

Fig. 5. (*continued*).

on the FPOA removal. Sections S4 to S5 had the greatest PFOA concentrations of 4.429 and 2.854 mg/kg, respectively, while S1 presented the lowest concentration of 0.312 mg/kg. These results indicate that most PFOA was electromigrated towards the cathode region.

Activated carbon is a highly porous material with a large surface area commonly used for adsorption of contaminants. The presence of iron on the AC can introduce additional properties and interactions compared to regular AC. PFOA interaction with FeAC can occur through several interactions:

1) Adsorption: FeAC and AC have high adsorption affinity for organic compounds due to their porous structure and large surface area. PFOA can be adsorbed onto the FeAC surface through electrostatic and hydrophobic interactions. The presence of iron on the surface can enhance the adsorption of PFOA due to the potential interaction between PFOA and iron.
2) Complexation: iron ions on the FeAC may interact with PFOA through complexation forming, forming Fe-PFOA complexes. This interaction can result in the immobilization of PFOA molecules, reducing their mobility and bioavailability.

The experimental data of these studies can be hypothesized that due to micro-electrolysis close to the FeAC PRB, PFOA formed a complex with Fe, thereby an electron transfer to the PFOA, which resulted in the formation of the following positively charged complex that had been migrated to the cathode.

$$C_7F_{15}COOH \xrightarrow{Fe^{3+}} [C_7F_{15}COOFe]^{2+} \quad (2)$$

PFOA degradation in the presence of Fe^{3+} in water treatment study resulted in the formation of $[C_7F_{15}COOFe]^{2+}$ complex through electron transfer from PFOA to Fe(III) (Liu et al., 2013). However, the mass balance of this study's analysis and the negligible concentration of intermediates demonstrated that PFOA was not degraded into small-chain compounds but interacted with the Fe to generate a net-positive complex. The migration of PFOA towards the cathode is assumed to have been caused by the generation of the complex mentioned above. The formation of ferric hydroxide close to the cathode, where hydroxide ions are continuously released by electrolysis reaction, may explain the apparent development of brown precipitate in sections S5-S6. The EK process with FeAC near the anode did not significantly improve the PFOA removal, as most PFOA was found near the cathode in the soil sections S4 and S5.

According to Table 3, the EK process with the FeAC PRB in the middle had the highest PFOA removal rate of 59.55 %, followed by the AC PRB with 52.35 % removal and regenerated AC PRB with 40.37 % removal. Placing the FeAC close to the anode in experiment T6 caused a sharp drop in PFOA removal efficiency to 21.96 %, with most of the PFOA accumulated in sections S4 and S5, circa 2.5 to 5 cm from the cathode (Fig. 4f). The movement of the PFOA-Fe complex towards the cathode region could be attributed to the sharp drop in removal rate where the PRB position was altered. In the unenhanced and AC-enhanced EK process, the electromigration of PFOA towards the anode was dominant.

Although experiment T3 had a higher removal rate than experiment T2, using a regenerated FeAC in the T5 experiment declined the PFOA removal efficiency from 59.55 % to 20.62 % (Table 3). Experiment T4 with a regenerated AC PRB had a higher % PFOA removal of 40.37 % than experiment T5 (20.61 %). Apparently, upon FeAC regeneration, the PFOA removal efficiency decreased dramatically, possibly related to the surface characteristics' failure to recover. As shown in Fig. 4g, the removal of PFOA in experiments T3 and T6 was relatively high in the soil sections close to the anode S1-S3 and lowest in S4 and S5, particularly in experiment T6. The significant difference in the removal rate of FeAC

Table 3
Mass Balance and Removal efficiency of EK tests.

Experiments	Initial PFOA in soil (mg)	Residual PFOA in treated soil (mg)	PFOA mass in PRB (mg)	PFOA mass in the electrolyte (mg)	PFOA mass in soil pore water (mg)	Mass balance (%)	PFOA removal (%)
T1	10	6.80	–	3.07	0.09	99.98	33.16 ± 0.11
T2	10	4.89	0.25	5.54	0.10	108.44	52.35 ± 0.42
T3	10	4.05	0.05	5.74	0.12	100.51	59.55 ± 0.01
T4	10	6.08	0.24	3.75	0.11	95.15	40.37 ± 0.21
T5	10	8.35	0.38	5.70	0.07	109.83	20.62 ± 0.42
T6	10	8.45	0.06	2.27	0.04	100.16	21.96 ± 0.75

PRB tests can be attributed to their position in the EK cell. As can be evident, PFOA migrated primarily towards the anode, and positioning the PRB at the anode did not substantially increase removal efficiency as a whole. PFOA removal in experiment T2 was lowest in sections S1–S2, then increasing towards section S6. According to the experimental data, the PFOA anion electromigrated towards the anode during the AC-PRB EK process, whereas the high PFOA concentration near the cathode in the EK experiments with FeAC PRB was due to the formation of a positively charged iron-PFOA complex that migrated towards the cathode. In a previous study, Fe-modified GAC outperformed GAC at adsorbing PFOA from an aqueous solution (Ahn et al., 2022). It was hypothesized that Fe-modified AC PRB would have a higher removal rate by adsorption mechanism. FeAC PRB enhanced the PFOA removal in this study, while PFOA adsorption onto the PRB was insignificant, according to the experimental data. Generally, PFOA removal in this study was lower than reported in the literature [39] due to its higher soil concentration and shorter EK duration.

Generally, PFOA will be soluble in water up to 9500 mg/L, which is much higher than the concentration of PFOA used in T1 to T6 experiments, 10 mg/L. PFOA will be transported by the electromigration mechanism from the cathode vicinity to the anode due to charge difference and from the anode vicinity to the cathode by the electroosmosis mechanism. The two transport mechanisms are responsible for the irregular distribution of PFOA across the soil, knowing that the PFOA distribution in the soil was further affected by the position of the PRB in the EK tests. Also, PFOA existed near the anode at higher concentrations than at the cathode due to the dominance of the electromigration transport mechanism during the EK process (Acar and Alshawabkeh, 1993).

In a previous study by (Niarchos et al., 2022), 89 % of PFAS was found within 5 cm of the anode after 21 days using 0.38 mA/cm2 (~30 mA) electric current across the soil specimen. This study detected 59 % and 52 % of PFOA in electrolytes and PRB of FeAC PRB-EK and AC PRB-EK tests at the end of 14 days of EK treatment at 20 mA electric current with a removal efficiency of about 98 % in soil sections close to the cathode. The better PFAS removal reported in the literature was due to the longer experimental time, higher applied electric current, and contaminant concentration in the soil. Also, in this study, PFOA represented PFAS contaminants in the soil compared to a range of PFAS compounds in the previous study (Niarchos et al., 2022). Also, this study used powdered activated carbon compared to granular activated carbon in Niarchos and co-workers' study. It should be noted that the accumulation of PFAS near the anode region in experiments T2, T4, and T5 was similar to that reported by the Niarchos team.

3.4. Characterisation of PRB

Subsequent analysis was conducted on AC and FeAC PRBs to validate the outcomes of the experiments. The surface characteristics and the efficacy of iron loading onto the AC were examined through scanning electron microscopy with energy-dispersive X-ray spectroscopy (SEM-EDS) before and after the coating process. Furthermore, the PRBs were analysed post-EK testing to corroborate the experimental observations, which indicated a loss of iron from the PRB after the EK test and, in the case of the regenerated FeAC PRB. Fig. 5b illustrates the presence of iron on the AC following the coating procedure. The iron coating on the AC decreased from 5.8 % to 3.3 % after the EK test. The iron concentration decreased after experiment T5, where the regenerated FeAC PRB was employed. These findings align with the experimental results and the removal efficiencies observed in the FeAC PRB tests.

Moreover, the specific surface area of activated carbon (AC) and iron-coated activated carbon (FeAC) was determined using BET measurements before and after the iron-coating process. A noticeable decrease in the surface area of AC was observed after iron loading, indicating successful surface impregnation. The AC surface area initially measured 1200 m^2/g, which subsequently decreased to 146.57 m^2/g following iron loading. This reduction in surface area after coating is consistent with previous studies that reported significant decreases in surface area upon iron impregnation (Suresh Kumar et al., 2017b). Furthermore, Fourier-transform infrared (FTIR) analysis confirmed surface modifications of the AC after iron coating. In the FTIR spectra of AC, FeAC before EK testing, and FeAC PRB after EK tests, distinct vibrational peaks were observed at 1650 cm^{-1}, 1100 cm^{-1}, and 670 cm^{-1}, corresponding to functional groups such as -C=O, -C-O, and -C-O-C- bending. Fig. 5d illustrates significant changes in peak intensity in the FTIR spectrum of FeAC PRB after coating. However, following the EK test, a decrease in intensity was observed, indicating the potential loss of iron from the PRB surface. The FTIR spectrum, ranging from 3900 to 600 cm^{-1}, captures the functional groups typically found in both organic and inorganic compounds. The FTIR spectrum of activated carbon (AC), represented by the blue line, shows relatively higher transmittance across the entire range, with notable peaks around 1600 cm^{-1} and 1100 cm^{-1}, indicating C═C stretching and C—O stretching vibrations, respectively. The spectrum of iron-coated activated carbon before the electrokinetic (EK) process, represented by the black line, shows a slight decrease in transmittance compared to AC, with changes around the 1600 cm^{-1} and 1100 cm^{-1} regions, suggesting chemical structure modifications due to the coating process. After the EK process, represented by the green line, the transmittance further reduces, with significant changes in peaks around 1600 cm^{-1} and 1100 cm^{-1}, indicating enhanced binding or transformation of functional groups. Detailed analysis reveals a minimal presence of hydroxyl or amine groups in the 3300–3500 cm^{-1} region and a low presence of aliphatic hydrocarbons in the 2900–3000 cm^{-1} region. The 1600 cm^{-1} peak decreases slightly after coating and EK process, suggesting interactions or transformations of structures. The 1400–1500 cm^{-1} region shows small peaks indicative of alkane structures. The 1100 cm^{-1} region, corresponding to C—O stretching, shows prominent peaks across all samples with intensity variations, indicating changes in oxygen-containing functional groups. Lastly, the 600–900 cm^{-1} region, indicating C—H bending and metal-oxygen bonds, shows distinct peaks, particularly in FeAC samples, suggesting metal-oxygen interactions due to the iron coating and EK process.

The variations in the Zeta potential of the permeable reactive barriers (PRBs) before and after the electrokinetic (EK) process are presented in Fig. 5c. At the end of the EK test, FeAC RFM exhibited an increased negative charge, which can be attributed to the loss of iron during the EK procedure. Conversely, the AC PRB showed a decrease in negativity after the EK test, possibly due to the adsorption of PFOA during the EK test or alterations in the pH of the PRB as a result of the acid front propagating in close proximity to the PRB zone during the EK tests (Fig. 3a).

3.5. AC and FeAC PRB performance

Activated carbon has been widely investigated as an adsorbent for removing PFOA from aqueous medium and stabilising soil remediation processes. It has been known as the best adsorbent for long-chain PFAS compounds. Due to the hydrophobic chain and hydrophilic head functional group of PFOA, hydrophobic interactions and electrostatic attractions serve as the primary adsorption mechanisms of AC (Jin et al., 2021). Molecular diffusion was identified as the crucial factor of PFOA adsorption onto powdered activated carbon (PAC), and the effectiveness of removing PFOA using PAC was about 99 % (Barth et al., 2021). PFOA accumulated in sections S1 and S2 in the AC PRB enhanced EK process, as depicted in Fig. 6a, indicating that electromigration is the predominant transportation mechanism in these tests.

In contrast, electroosmotic flow towards the cathode explains the presence of PFOA near the cathode region in the AC-EK tests. Also, PFOA was adsorbed onto the AC PRB due to its affinity to AC media. Near the cathode, where OH is constantly released due to water electrolysis causing soil pH increase, a high PFOA leachability occurred in the soil.

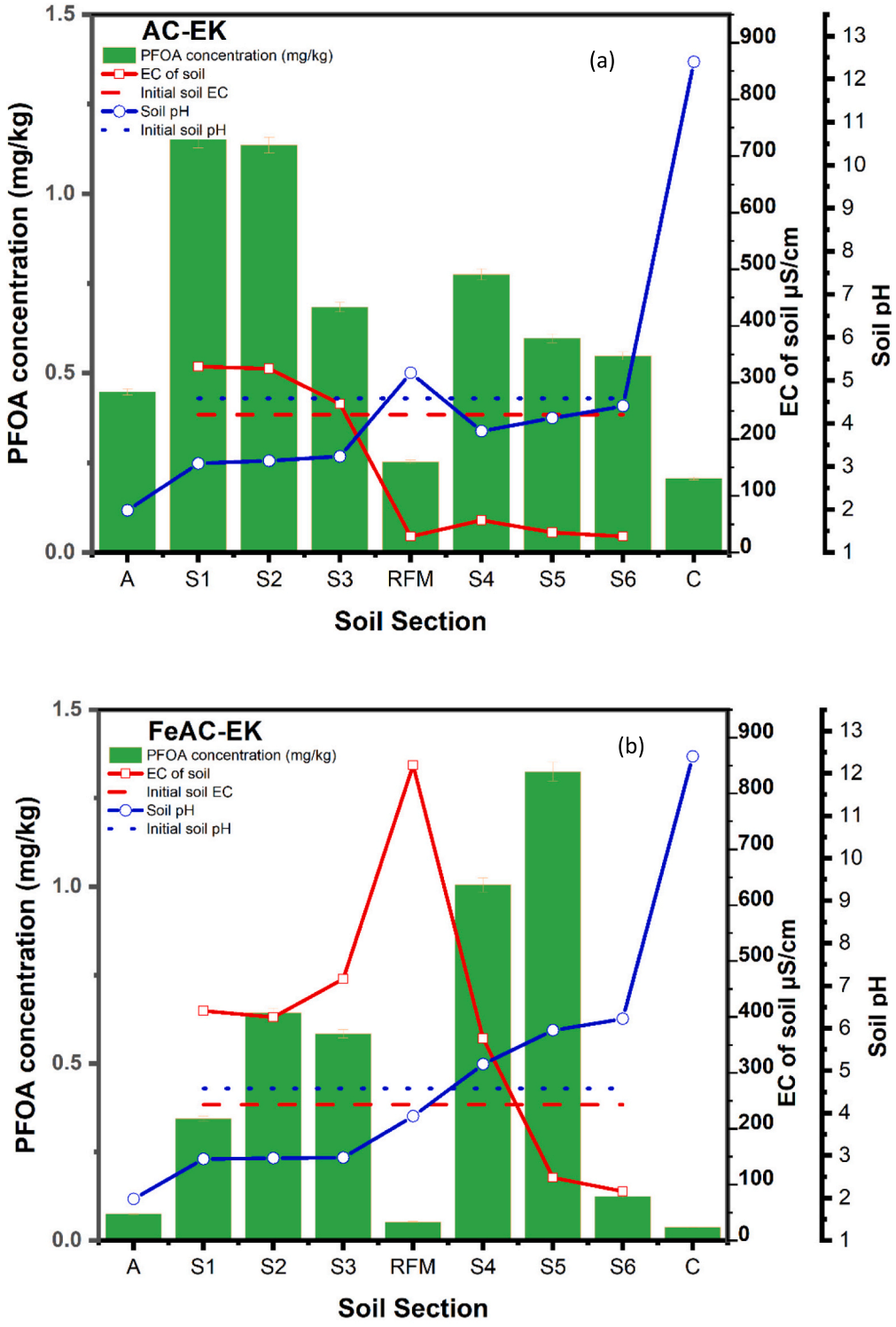

Fig. 6. (a) AC-PRB EK test; (b)AC PRB EK tests.

Therefore, the concentration of PFOA is less in the soil section close to the cathode. However, as shown in Fig. 6b, PFOA was transported towards sections S4 and S5, and the concentration of PFOA is less in soil sections near the anode. Contrary to the AC PRB test, most PFOA was transported to the cathode in the FeAC PRB test. This phenomenon can be hypothesized that PFOA forms a complex with Fe^{3+}, favouring the transportation towards the cathode.

As depicted in Fig. 6a and b, the change in pH and EC also differ in both tests. FeAC PRB exhibits higher EC than AC PRB, which can be attributed to the loading of Fe onto the AC. Moreover, the soil pH is higher in sections S3 to S6 of the FeAC EK test, which is above the initial pH level. The precipitation of iron compounds at alkaline pH near the cathode could explain the higher pH in the FeAc tests. In contrast, the pH was higher in S3 to S6 of the AC PRB EK but remained below the initial pH value.

3.6. Energy consumption and EOF

Specific power consumption E_u (kWh kg^{-1}) was determined using Eq. 3 while considering remediation efficiency.

$$E_u = \frac{10^{-3}}{V_s}\int_0^t VIdt \quad (3)$$

where V_s is the total amount of treated soil (kg), V is the applied voltage (V), I is electric current (A), and t is the treatment time (h).

The specific energy consumption varied from 0.037 kWh kg^{-1} in experiment T5 to 0.076 kWh kg^{-1} in experiment T6. As the average electric current of the EK process increased, so did the specific energy consumption of the EK process. However, as shown in Fig. 7, PFOA removal efficiency was not directly proportional or correlated with energy consumption (kWh kg^{-1}). High removal efficiency did not require higher energy consumption. As shown in Fig. 7, the conventional EK process in experiment T1 consumed high SEC for soil treatment, which could be attributed to the higher soil resistivity and the voltage applied in the test. Compared to PRB-enhanced EK tests, the constant current of experiment T1 dropped rapidly and reached the maximum voltage in a shorter time. As a result, the voltage remained constant at a higher value for longer. Compared to all EK tests, the EK process with the FeAC PRB at the anode (experiment T6) consumed the highest electrical energy because experiment T6 had the longest elapsed constant current among all the tests; hence, the average current for this test was the highest.

The highest average current resulted in the highest SEC in the EK treatment. The higher average current can be attributed to the presence and migration of the Fe to the cathode. This observation is consistent with the previous experimental results. Experiment T3, with the highest removal rate, had 0.689 kWh kg^{-1} SEC, whereas experiment T2 had a slightly lower SEC of 0.585 kWh kg^{-1}. This is attributed to the prolonged constant current with increased elapsed time in experiment T3 compared to experiment T2, which resulted in a greater average current for the test.

The variation in electroosmotic flow (EOF) in EK tests is presented in Fig. 7. To demonstrate the relationship between the variation of the EOF with energy consumption and overall removal rate. EOF depends on the fluid characteristics (dielectric constant and viscosity) and soil surface characteristics such as zeta potential and voltage gradient (Cameselle, 2015). The cumulative EOF was collected and measured at the end of the experiment. The removal rate of PFOA post-remediation was not closely correlated with the EOF and the specific energy consumption (SEC), as seen in Fig. 7. For all experiments, EOF was generally high at the start of the EK test. It is explained by the ion production brought on by the electrolysis reaction at the electrode at the beginning of the EK test. Depending on the PRB applied, within the first 24 h, 350–400 mL of EOF were generated and gradually declined over time. The EOF in experiment T1 started high before dropping sharply and producing the lowest EOF. This outcome may be related to the sharp decline in electric current in experiment T1, which slowed the EOF. In experiments T2 and T3, the increased EOF can be attributed to the longer constant current and high average voltage. In experiment T3, the constant current was stable for longer than in experiment T2. However, the maximum EOF was found in experiment T4 with a recycled AC, probably due to the high average voltage and the changing zeta potential of the PRB. Experiment T5 EOF decreased drastically, which can also be attributed to the change in voltage and zeta potential of recycled FeAC PRB after regeneration. Although experiment T6 had a longer constant current during the remediation process, the EOF was low due to the increased soil resistivity and the accumulation of PFOA in the soil sections near the cathode.

4. Conclusion

Based on mass balance and negligible concentration of intermediates in the soil section, it can be hypothesized that PFOA has not been degraded into shorter chain PFAS but is more likely transported and adsorbed onto the PRB in the EK test. The negligible concentration of other intermediates refers to concentrations that were so low that they were considered insignificant or almost non-existent. The transportation of PFOA and accumulation in the sections near the anode in the AC PRB EK test and the accumulation of PFOA near the cathode region in the FeAC PRB EK test suggest the transportation mechanism in these tests was different. In the enhanced AC-EK process, PFOA is transported towards the anode by electromigration and towards the cathode by electroosmosis. FeAC EK tests hypothesized that PFOA formed a complex with Fe, resulting in their transportation to the cathode region. FeAC PRB enhanced EK test where PRB was placed in the middle of the EK cell resulted in 59 % overall PFOA removal, whereas AC PRB enhanced EK test resulted in 54 % removal. In general, results showed a maximum of 0.4 mg/L PFOA was captured in the new AC or FeAC PRBs and 0.3 mg/L

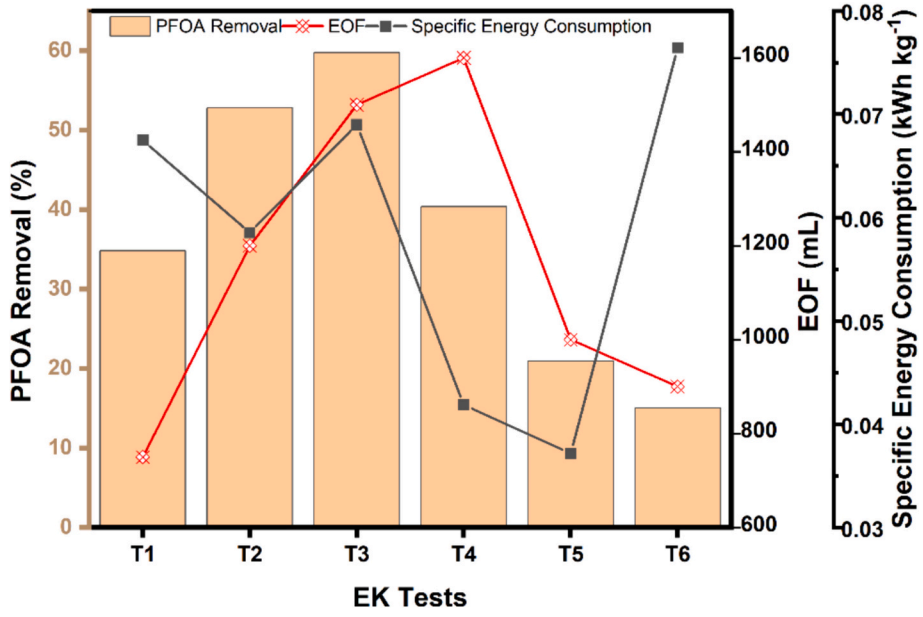

Fig. 7. Specific Energy Consumption (kWh kg^{-1}), total PFOA removal of all EK tests and variation of EOF.

in the regenerated AC or FeAC PRBs.

Several recommendations for future research have emerged based on the experimental results obtained in this study. Firstly, it is suggested that further investigations should be conducted to perform real soil testing using the biosurfactant-enhanced electrokinetic process coupled with AC/FeAC permeable reactive barriers. These tests will allow for an assessment of the technique's performance and efficacy. A pilot plant study on real PFAS-contaminated soil treatment by the PRB-Ek system is recommended to evaluate the process efficiency in real life. Also, future work must investigate the PRB-EK system efficiency for the treatment of short-chain and other long-chain PFAS compounds. It is noteworthy that FeAC PRB loses its effectiveness for PFOA adsorption after regeneration, and hence, it is not recommended for reuse.

Additionally, it is advisable to explore the effects of different PRB configurations, such as those employing nano zero-valent iron (nZVI), iron oxide, or other nanomaterials, to determine their impact on the removal of *per*- and polyfluoroalkyl substances (PFAS) from contaminated soil. Furthermore, future studies should encompass a wider range of PFAS compounds and consider pilot-scale investigations to understand the technique's applicability and effectiveness comprehensively.

CRediT authorship contribution statement

Namuun Ganbat: Writing – original draft, Investigation, Formal analysis, Data curation, Conceptualization. **Ali Altaee:** Writing – original draft, Visualization, Validation, Supervision, Resources, Data curation, Conceptualization. **Faris M. Hamdi:** Validation, Investigation, Formal analysis, Data curation, Conceptualization. **John Zhou:** Writing – original draft, Validation, Supervision, Formal analysis, Conceptualization. **Mahedy Hasan Chowdhury:** Writing – original draft, Validation, Formal analysis, Data curation. **Syed Javaid Zaidi:** Writing – original draft, Formal analysis, Data curation. **Akshaya K. Samal:** Validation, Investigation, Data curation. **Raed Almalki:** Writing – review & editing, Formal analysis, Data curation. **Marie Joshua Tapas:** Formal analysis, Data curation.

Declaration of competing interest

The authors declare that they have no known competing financial interests or personal relationships that could have appeared to influence the work reported in this paper.

Data availability

Data will be made available on request.

Acknowledgement

This research is made possible by a food security research award (MME04-0607-230061) from the Qatar National Research Fund (QNRF) in partnership with the Ministry of Municipality. The statements made herein are solely the responsibility of the authors.

References

Acar, Y.B., Alshawabkeh, A.N., 1993. Principles of electrokinetic remediation. Environ. Sci. Technol. 27 (13), 2638–2647.
Ahn, S.-K., Park, K.-Y., Song, W.-j., Park, Y.-m., Kweon, J.-H., 2022. Adsorption mechanisms on perfluorooctanoic acid by FeCl3 modified granular activated carbon in aqueous solutions. Chemosphere 303, 134965.
Altaee, A., Smith, R., Mikhalovsky, S., 2008. The feasibility of decontamination of reduced saline sediments from copper using the electrokinetic process. J. Environ. Manag. 88 (4), 1611–1618.
Altarawneh, M., Almatarneh, M.H., Dlugogorski, B.Z., 2022. Thermal decomposition of perfluorinated carboxylic acids: kinetic model and theoretical requirements for PFAS incineration. Chemosphere 286, 131685.
Andrade, D.C., dos Santos, E.V., 2020. Combination of electrokinetic remediation with permeable reactive barriers to remove organic compounds from soils. Curr. Opin. Electrochem. 22, 136–144.
Barth, E., McKernan, J., Bless, D., Dasu, K., 2021. Investigation of an immobilization process for PFAS contaminated soils. J. Environ. Manag. 296, 113069.
Brusseau, M.L., Anderson, R.H., Guo, B., 2020. PFAS concentrations in soils: background levels versus contaminated sites. Sci. Total Environ. 740, 140017.
Cameselle, C., 2015. Enhancement of electroosmotic flow during the Electrokinetic treatment of a contaminated soil. Electrochim. Acta 181, 31–38.
Chen, W., Parette, R., Zou, J., Cannon, F.S., Dempsey, B.A., 2007. Arsenic removal by iron-modified activated carbon. Water Res. 41 (9), 1851–1858.
Cheng, M., Zeng, G., Huang, D., Yang, C., Lai, C., Zhang, C., et al., 2017. Advantages and challenges of tween 80 surfactant-enhanced technologies for the remediation of soils contaminated with hydrophobic organic compounds. Chem. Eng. J. 314, 98–113.
Epa Au, N.Z., 2019. PFAS National Environmental Management Plan Version 2.0 Consultation Draft.
European C, 2020. Regulation (EU) 2019/1021 of the European Parliament and of the Council of 20 June 2019 On persistent organic pollutants. PFOA has been listed in Annex I of the POPs Regulation with Regulation (EU) 2020/784, 2020(793), pp. 1–5.
European C, 2020. Poly- and perfluoroalkyl substances (PFAS): Chemicals Strategy for Sustainability Towards a Toxic-Free Environment. Commission Staff Working Document, pp. 1–22.
Figueroa, A., Cameselle, C., Gouveia, S., Hansen, H.K., 2016. Electrokinetic treatment of an agricultural soil contaminated with heavy metals. J. Environ. Sci. Health A Tox. Hazard. Subst. Environ. Eng. 51 (9), 691–700.
Ganbat, N., Altaee, A., Zhou, J.L., Lockwood, T., Al-Juboori, R.A., Hamdi, F.M., et al., 2022. Investigation of the effect of surfactant on the electrokinetic treatment of PFOA contaminated soil. Environ. Technol. Innov. 28, 102938.
Ganbat, N., Hamdi, F.M., Ibrar, I., Altaee, A., Alsaka, L., Samal, A.K., et al., 2023. Iron slag permeable reactive barrier for PFOA removal by the electrokinetic process. J. Hazard. Mater. 460, 132360.
Ghobadi, R., Altaee, A., Zhou, J.L., McLean, P., Ganbat, N., Li, D., 2020. Enhanced copper removal from contaminated kaolinite soil by electrokinetic process using compost reactive filter media. J. Hazard. Mater. 402, 123891.
Ghobadi, R., Altaee, A., Zhou, J.L., Karbassiyazdi, E., Ganbat, N., 2021. Effective remediation of heavy metals in contaminated soil by electrokinetic technology incorporating reactive filter media. Sci. Total Environ. 794, 148668.
Guedes, P., Lopes, V., Couto, N., Mateus, E.P., Pereira, C.S., Ribeiro, A.B., 2019. Electrokinetic remediation of contaminants of emergent concern in clay soil: effect of operating parameters. Environ. Pollut. 253, 625–635.
Hahladakis, J.N., Latsos, A., Gidarakos, E., 2016. Performance of electroremediation in real contaminated sediments using a big cell, periodic voltage and innovative surfactants. J. Hazard. Mater. 320, 376–385.
Hou, J., Li, G., Liu, M., Chen, L., Yao, Y., Fallgren, P.H., et al., 2022. Electrochemical destruction and mobilization of perfluorooctanoic acid (PFOA) and perfluorooctane sulfonate (PFOS) in saturated soil. Chemosphere 287 (P3), 132205.
Jin, T., Peydayesh, M., Mezzenga, R., 2021. Membrane-based technologies for per- and poly-fluoroalkyl substances (PFASs) removal from water: removal mechanisms, applications, challenges and perspectives. Environ. Int. 157, 106876.
Kim, H.C., Lee, C.G., Park, J.A., Kim, S.B., 2010. Arsenic removal from water using iron-impregnated granular activated carbon in the presence of bacteria. J. Environ. Sci. Health - Part A Toxic/Hazard. Subst. Environ. Eng. 45 (2), 177–182.
Lenka, S.P., Kah, M., Padhye, L.P., 2021. A review of the occurrence, transformation, and removal of poly- and perfluoroalkyl substances (PFAS) in wastewater treatment plants. Water Res. 199, 117187.
Li, Z., Yuan, S., Wan, J., Long, H., Tong, M., 2011. A combination of electrokinetics and Pd/Fe PRB for the remediation of pentachlorophenol-contaminated soil. J. Contam. Hydrol. 124 (1), 99–107.
Liu, D., Xiu, Z., Liu, F., Wu, G., Adamson, D., Newell, C., et al., 2013. Perfluorooctanoic acid degradation in the presence of Fe(III) under natural sunlight. J. Hazard. Mater. 262, 456–463.
Mahinroosta, R., Senevirathna, L., 2020. A Review of the Emerging Treatment Technologies for PFAS Contaminated Soils. Academic Press, p. 109896.
Mena, E., Villaseñor, J., Rodrigo, M.A., Cañizares, P., 2016. Electrokinetic remediation of soil polluted with insoluble organics using biological permeable reactive barriers: effect of periodic polarity reversal and voltage gradient. Chem. Eng. J. 299, 30–36.
Niarchos, G., Sörengård, M., Fagerlund, F., Ahrens, L., 2022. Electrokinetic remediation for removal of per- and polyfluoroalkyl substances (PFASs) from contaminated soil. Chemosphere 291, 133041.
Niarchos, G., Ahrens, L., Kleja, D.B., Leonard, G., Forde, J., Bergman, J., et al., 2023. In-situ application of colloidal activated carbon for PFAS-contaminated soil and groundwater: a Swedish case study. Remediat. J. 33 (2), 101–110.
Oliver, D.P., Li, Y., Orr, R., Nelson, P., Barnes, M., McLaughlin, M.J., et al., 2019. The role of surface charge and pH changes in tropical soils on sorption behaviour of per- and polyfluoroalkyl substances (PFASs). Sci. Total Environ. 673, 197–206.
Ren, D., Li, S., Wu, J., Fu, L., Zhang, X., Zhang, S., 2019. Remediation of Phenanthrene-contaminated soil by Electrokinetics coupled with Iron/carbon permeable reactive barrier. Environ. Eng. Sci. 36 (9), 1224–1235.
Ruiz, C., Mena, E., Cañizares, P., Villaseñor, J., Rodrigo, M.A., 2014. Removal of 2,4,6-Trichlorophenol from spiked clay soils by Electrokinetic soil Flushing assisted with granular activated carbon permeable reactive barrier. Ind. Eng. Chem. Res. 53 (2), 840–846.
Sugioka, H., Matsuoka, K., Moroi, Y., 2003. Temperature effect on formation of sodium cholate micelles. J. Colloid Interface Sci. 259 (1), 156–162.
Sun, Y., Gao, K., Zhang, Y., Zou, H., 2017. Remediation of persistent organic pollutant-contaminated soil using biosurfactant-enhanced electrokinetics coupled with a zero-valent iron/activated carbon permeable reactive barrier. Environ. Sci. Pollut. Res. 24 (36), 28142–28151.

Suresh Kumar, P., Prot, T., Korving, L., Keesman, K.J., Dugulan, I., van Loosdrecht, M.C. M., et al., 2017a. Effect of pore size distribution on iron oxide coated granular activated carbons for phosphate adsorption – importance of mesopores. Chem. Eng. J. 326, 231–239.

Suresh Kumar, P., Prot, T., Korving, L., Keesman, K.J., Dugulan, I., van Loosdrecht, M.C. M., et al., 2017b. Effect of pore size distribution on iron oxide coated granular activated carbons for phosphate adsorption – importance of mesopores. Chem. Eng. J. 326, 231–239.

Turner, L.P., Kueper, B.H., Jaansalu, K.M., Patch, D.J., Battye, N., El-Sharnouby, O., et al., 2021. Mechanochemical remediation of perfluorooctanesulfonic acid (PFOS) and perfluorooctanoic acid (PFOA) amended sand and aqueous film-forming foam (AFFF) impacted soil by planetary ball milling. Sci. Total Environ. 765, 142722.

Virkutyte, J., Sillanpää, M., Latostenmaa, P., 2002. Electrokinetic soil remediation — critical overview. Sci. Total Environ. 289 (1), 97–121.

Yan, D., Gang Daniel, D., Zhang, N., Lin, L., 2013. Adsorptive selenite removal using Iron-coated GAC: modeling selenite breakthrough with the pore surface diffusion model. J. Environ. Eng. 139 (2), 213–219.

Zhan, J., Zhang, A., Héroux, P., Guo, Y., Sun, Z., Li, Z., et al., 2020. Remediation of perfluorooctanoic acid (PFOA) polluted soil using pulsed corona discharge plasma. J. Hazard. Mater. 387, 121688.

Zhou, H., Xu, J., Lv, S., Liu, Z., Liu, W., 2020. Removal of cadmium in contaminated kaolin by new-style electrokinetic remediation using array electrodes coupled with permeable reactive barrier. Sep. Purif. Technol. 239, 116544.